Journal of Applied Fluid Mechanics, Vol. 17, No. 5, pp. 1099-1111, 2024.
Available online at www.jafmonline.net, ISSN 1735-3572, EISSN 1735-3645.
https://doi.org/10.47176/jafm.17.05.2217

Enhancement of Jet Mixing using Stepped Tandem Tabs

S. Venkatramanan[1], S. Thanigaiarasu[2†] and M. Kaushik[3]

[1] *Department of Aeronautical Engineering, KCG College of Technology, Chennai, Tamil Nadu, 600 097, India*
[2] *Department of Aerospace Engineering, MIT Campus, Anna University, Chennai, Tamil Nadu, 600 044, India*
[3] *Department of Aerospace Engineering, Indian Institute of Technology, Kharagpur, West Bengal, 721 302, India*

†Corresponding Author Email: sthanigaiarasu@mitindia.edu

ABSTRACT

Mixing characteristics of jet emerging from a subsonic nozzle exit has been experimented and the results are compared with uncontrolled jet and controlled jet configurations. The mixing enhancement was achieved using a passive method of jet control in which tandem tabs arrangement with rectangular cross section are fixed at the nozzle exit. Two Tab configurations, the Tandem tab (TT) and Stepped Tandem Tab (STT) are used to enhance the mixing characteristics of the jet, the aspect ratio (length /width) of the tabs was 1.67 offering a blockage ratio of 9.55% to the nozzle exit. The blockage ratio of TT and STT configurations are maintained to be equal so that the mixing characteristics can be compared. The axial and radial jet spread are compared for nozzle exit Mach numbers of 0.6, 0.8 and 1.0. The TT controlled jet offered a potential core reduction of 63%, 78% and 82% for Mach numbers 0.6, 0.8 and 1.0 respectively. The STT controlled jet offered a potential core reduction of 89%, 90% and 85% for Mach numbers 0.6, 0.8 and 1.0 respectively. The radial spread of uncontrolled jet, controlled jet with TT and STT are plotted at several X/D locations and found that the controlled jets have more jet spread in both radial directions. A simulation is conducted for jets with exit Mach number 0.8 and the results are validated with the experimental findings. Based on the preliminary experimentation and computation, the STT controlled jet achieved better jet mixing through more potential core reduction and radial spread characteristics as compared to the TT configuration and base nozzle.

Article History

Received August 9, 2023
Revised November 30, 2023
Accepted December 11, 2023
Available online February 24, 2024

Keywords:

Jet mixing
Mass entrainment
Potential core
Uncontrolled jet
Tandem tab
Stepped tandem tab

1. INTRODUCTION

The mixing enhancement in jets has various applications, such as noise reduction in jet exhaust, material deposition and effective combustion. The vast area of application provides a platform for the creation of innovative designs and techniques. The jet mixing techniques are broadly classified as active and passive controls. The jet control using the active method involves the application of external energy for enhancing the jet mixing. The passive methods rather require only geometric variations to enhance the jet mixing. The passive method created better mixing efficiency and can be employed with ease in any nozzle configuration. The passive methods also involve the use of a secondary body that acts as vortex generator. The diametrically opposed pair of tabs fixed at nozzle exit is a passive method of jet control. These tabs create pair of counter rotating vortices which change into streamwise vortices and travel downstream.

Bradbury and Khadem (1975) were the first to experiment with the effect of tabs in jet development. The distortion of the jet was created by the tabs fixed at the exit of the nozzle. The tab facing the flow from the nozzle exit creates a pressure hill which becomes the source for the generation of vortices in the jet.

Ahuja and Brown (1989) conducted a wide range of experimental studies on the enhancement of jet mixing using tabs at various locations and numbers. They also concluded that the effect of tabs on decay characteristics of hot and cold jets was not significantly different.

The tab geometry was varied to achieve enhancement in jet mixing. Zaman et al. (1992) measured the thrust loss caused due to the delta tabs placed at the nozzle exit. The findings also concluded that the thrust loss is 3 percentage for delta tabs and the tab does not work in over-expanded conditions. Zaman et al. (1994) investigated the delta tabs that act as vortex generators creating pair of counter-rotating streamwise vortices. It

NOMENCLATURE

TT	Tandem Tab	M_j	nozzle exit Mach number
STT	Stepped Tandem Tab	X	measurement along X directions
D	nozzle exit diameter	Y	measurement along Y directions
M	local Mach number	Z	measurement along Z directions
k	turbulence kinetic energy	U	mean velocity
σ	turbulent Prandtl number	ν_T	kinematic eddy viscosity
S	strain rates scalar	d	distance from the closest surface

was found that the delta tabs are better efficient in jet mixing and also have the benefit of less blockage to the nozzle exit.

Samimy et al. (1993) measured the noise fields of axisymmetric jets and found that the four tab configuration reduced the noise level by 6 dB compared to free jet. Their experiments also revealed that the jet centerline velocity decay is a measure of more jet spread. The schlieren images of the supersonic jet revealed the jet bifurcation due to tabs.

Zaman (1993) experimented with the effect of delta tabs on mixing enhancement and found that the local pressure hill ahead of the tab and the vortex filament shed from the corners of the tabs are the two sources for the generation of the streamwise vortices. Gretta and Smith (1993) illustrated that the low speed fluids are transported into the high speed fluids using counter rotating vortices generated in the wake region of a passive mixing tab.

Bohl and Foss (1996) investigated the effect of secondary tabs in addition to the primary tabs and found that the additional tabs increase the rate of mixing and enhance the benefits of a single tab.

Rathakrishnan (2012) visualized the twin vortex behind a flat plate and calculated the length of reverse flow for increasing Reynolds number.

Auteri et al., (2008) investigated the effect of tandem flat plates placed normal to the flow. The study focused on identifying the ideal distance between two plates and its role in the vortex generation. The plates separated by a distance equal to the chord are efficient for better vortex creation. Thanigaiarasu et al. (2008) used arc shaped tabs in facing in and out orientation and found that the arc tab facing created a maximum of 80% reduction in the potential core length. Singh and Rathakrishnan (2002) experimented with the effect of tabs on the decay characteristics of jets and justified that the tabs were more effective for under expanded jet than the correctly expanded jets. Lovaraju et al. (2004) increased the mixing in supersonic jet with the shifted cross wire attached to the nozzle. The influence of shifting the cross wire was found to reduce the potential core length by 30% at Mach 1.8.

The need for reducing the tab blockage to the nozzle exit, perforated tabs was found high commendable. Dharmahinder et al. (2011) investigated the effect of perforated arc-tabs on jet mixing and found the perforated arc-tabs are efficient in jet control reducing the core length by a maximum of 62% for subsonic jets and 75% for correctly expanded Mach 1 jet with reduced blockage leading to the minimum thrust loss. Ahmad et al. (2013) modified the perforation on tabs to be inclined. The simulation results for slanted perforation of 10^0 show better jet mixing. Ahmad et al. (2015) show an experimental study of the enhancement of jet mixing with slanted perforated tabs for subsonic and transonic jets. The 30^0 inclined perforation was efficient and achieved 55% reduction in potential core length.

Maruthupandiyan and Rathakrishnan (2016) extended the work shifted tabs and experimented with the jet control for supersonic conditions. The shifted tabs created superior mixing characteristics in comparison to tabs located at the nozzle exit.

Alam et al. (2016) conducted an extensive study on the vortex creation from the tandem cylinders by varying the separation distance and incidence angle. The study addressed the flow phenomenon of vortex generation and interactions between the upstream and downstream objects.

Jabez Richards et al. (2023) used asymmetric tab configuration to enhance the mixing characteristics of the jet. The asymmetric jet mixing has the advantage of enhanced mixing and has applications in jet thrust vectoring.

Thanigaiarasu et al. (2023) numerically investigated the vane-shaped vortex generators and the mixing characteristics for subsonic jets. These vanes are capable of increasing jet mixing with minimum pressure loss.

The previous studies indicate the wide use of a single tab with geometric modifications in controlling the jets. The presence of more number of tabs is found to increase the jet mixing but it subsequently increases the nozzle blockage and thrust loss. The wide range of earlier research emphasizes better mixing enhancement, thus urging the need for the creation of better tab configurations. Therefore, the innovation of tab configurations with better mixing capabilities with minimum blockage to the nozzle exit is preferable. The present experimentation of jet control is to investigate the effect of tandem tabs. The tandem tabs are solid tabs arranged one behind the other attached to the nozzle exit. The literature review reveals that limited work on usage of tandem tab configurations as much of the work was carried out with single tab configurations. In the present study, the investigation focuses on the control of jets at subsonic and sonic correctly expanded conditions. Two types of tandem tab configurations with the same nozzle blockage ratio are experimented in this study. In one configuration, the first and second tab has the same height and in the second configuration, the stepped

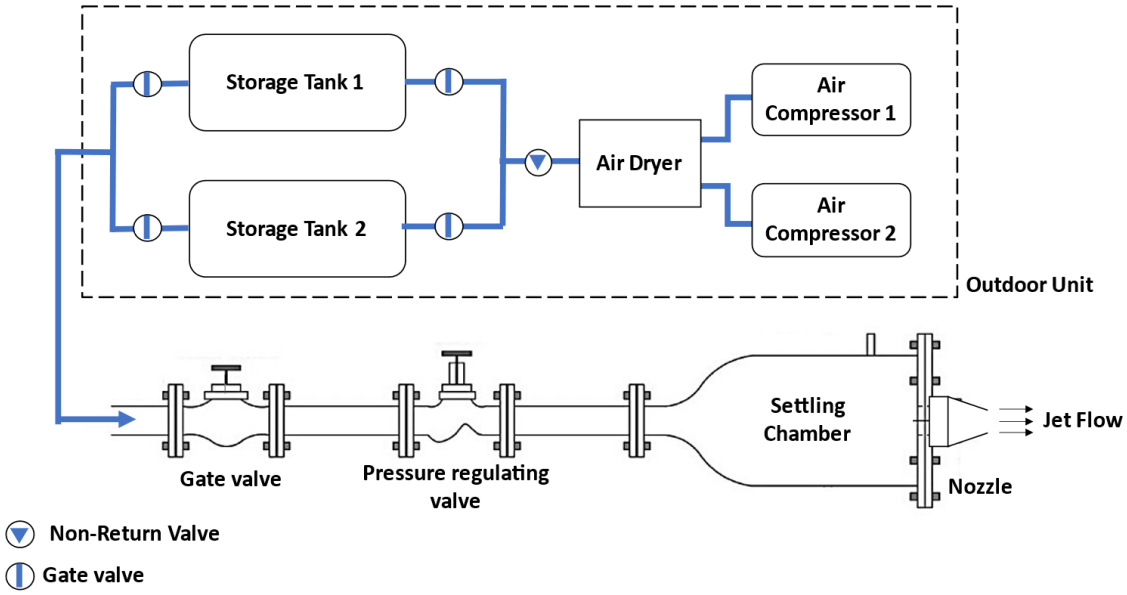

Fig. 1(a) Schematic diagram of high-speed jet facility

Fig. 1(b) Photographic view of the facility

tandem tabs (STT) of different heights were used. In the stepped tandem tabs configuration, the height of the second tab is twice the height of the first tab. In TT configuration, the first tabs face the flow from the nozzle exit and the second tab is in the wake region of the first tab. In STT Configuration, the reduction in height of the first tab allows the subsequent amount of flow to the second tab. The formation of a pressure hill in TT is expected to happen only in the first tab whereas in the STT, the pressure hill may form on both the first and second tab as the height of the tabs are different. The multiple pressure hill formed in STT is expected to create more vortices in the flow and may increase the mixing of the jet. The experimental investigation of the mixing characteristics of the uncontrolled, TT and STT Controlled jets for the jet Mach numbers of 0.4, 0.6 and 1.0 are presented in the current study.

2. EXPERIMENTAL METHODOLOGY

The jet centerline Mach number decay and the jet spread in radial directions are the measures used to understand the enhancement of jet mixing. The experimentation involves the use of a free jet facility, a suitable nozzle model, pitot tubes and data acquisition systems.

2.1 Free Jet Facility

The experiments were conducted at high-speed Jet facility Laboratory, MIT Campus, Anna University to generate a jet flow of desired Mach numbers 0.6, 0.8 and 1.0. The outdoor unit of the facility consists of two air compressors used to compress the atmospheric air and the moisture is removed using an air dryer. The dry pressurized air is stored in two storage tanks with a capacity of 4000 liters and capable of withstanding 20 Bar pressure. The high-pressure air entering the free jet facility is controlled using a gate valve and a pressure regulating valve. The desired settling chamber pressure is achieved by expanding the air in a wide-angle diffuser section. The nozzle exit is open to the stagnant air at the laboratory and the total pressure required at the settling chamber is maintained for the required Mach number at the nozzle exit.

The subsonic nozzle made of brass is attached to the settling chamber using a threaded coupling unit. A convergent nozzle with a circular cross-section having 40mm inlet diameter and 20mm exit diameter with a convergent angle of 11.3 degrees was used to accelerate the flow. The schematic view and a photograph of the jet facility are shown in Fig. 1 (a) and Fig. 1 (b).

Fig. 2(a) Photographic view of Uncontrolled, TT Controlled and STT controlled Nozzle configurations

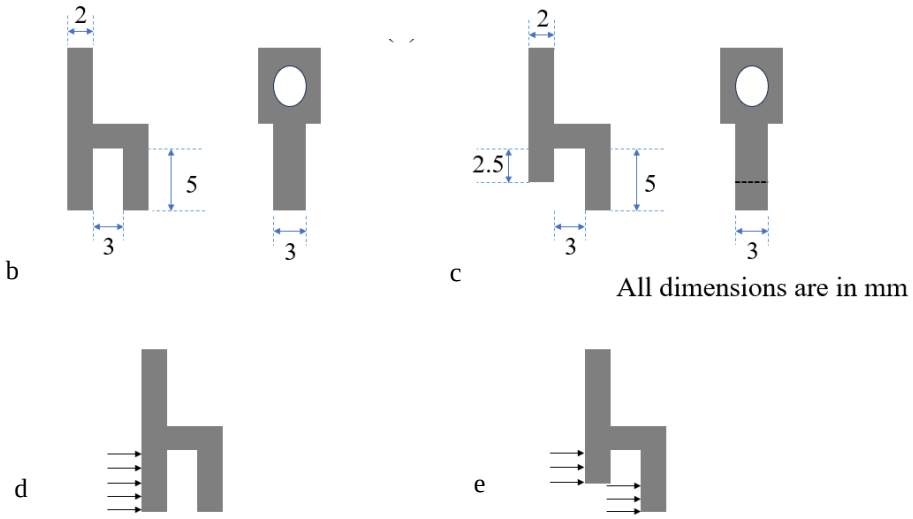

Fig. 2 Schematich Schetch of (b) TT configuration, (c) STT configuration, (d) Pressure hill formation in TT configuration and (e) Pressure hill formation in STT configuration

The pitot pressure is measured at various downstream locations of the jet using a pitot probe. The pitot probe is mounted to the 3-dimensional traverse mechanism capable of moving 30 times the nozzle exit diameter in all three directions. The traverse mechanism ensures accurate location with a minimum transition of 0.1mm. The pitot probe is placed normal to the flow with the measuring port facing the flow and the pitot pressure measured is converted to equivalent flow Mach number considering the isentropic flow conditions. The pitot probe has a 0.4 mm internal diameter and 0.6 mm of outer diameter. The ratio of the probe area to the nozzle exit area is $0.9*10^{-3}$ which is below the ideal value of $15*10^{-3}$.

2.2 Concept of TT and STT Jet Control

Two pair of tabs are fixed diametrically opposite at the nozzle exit. Each tab in the pair creates a pair of counter-rotating vortices which increases the mass entrainment from the atmosphere into the core jet, thus promoting the jet mixing. Figure 2(a) shows the three nozzle configurations used for the experimentation of jet mixing. The present study limits the study of the effect of TT and STT on jet mixing shown in Fig. 2 (b) – (c). The TT is two identical rectangular tabs arranged one behind the other separated by a distance of 3 mm from the first tab which is fixed at the nozzle exit, the tab facing the flow has 5 mm height, 3 mm width and 2 mm thickness. The stepped tandem tab has a reduced height of 2.5 mm for the first tab facing the flow and all other dimensions remain the same as that of the tandem tab. Figure 2(d) shows the predicted single pressure hill formation in TT and in Fig. 2(e) the STT configuration results in the creation of two separate pressure hills in each tab. The pressure hill created in each tab surface becomes the source of the vortex generation downstream.

2.3 Instrumentation

The total pressure at the settling chamber and the pitot pressure are measured using a 16-channel pressure transducer. The pressure scanner is a differential type with a measuring range of 0-20 bar (0-300psi) and an accuracy of $0.7*10^{-5}$ bar (0.01 psi). The sampling rate of the scanner is 300 samples per second, therefore the pressure measured is a mean pitot pressure. The pressure measured at all locations is found to be repeatable within ±3%.

3. Result and Discussion

The nozzle exit diameter is used to nondimensionalize all locations in three axes. The jet axis is the line originating from the center of the nozzle exit and extends downstream. The coordinate system used for the measurement is shown in the Fig.3. The axial locations along the jet axis are represented as X/D a

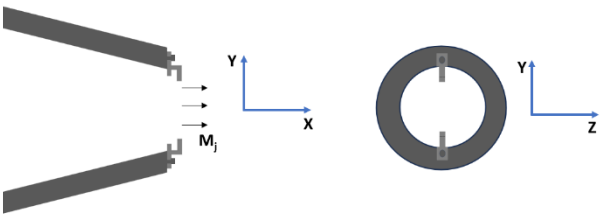

Fig. 3 Nozzle fitted with the STT and the coordinate system

ratio of the axial distance from the nozzle exit to the nozzle exit diameter. The radial locations along the tab direction are represented as Y/D, a ratio of radial distance from the jet axis to the nozzle exit diameter. Similarly, the radial locations normal to the tab are defined as Z/D measured from the jet axis.

The measured Mach number (M) at any location is nondimensionalized using the nozzle exit Mach number (M_j). The Mach number at any location is represented as M/M_j.

3.1 Centerline Mach Decay

The jet decay along the centerline or the jet axis is a measure to determine the mixing effectiveness of the jet. The centerline Mach decay plotted along X/D states the extent of potential core length and the jet decay characteristics of the jet. The centerline Mach decay of TT and STT controlled jets are compared with the uncontrolled jet. The centerline Mach decay comparison of TT and STT controlled jets with the uncontrolled jet for Mj=0.6 is shown in the Fig.4 (a).

The potential core length of the jet controlled with TT and STT were 1.75D and 0.5D respectively. From Fig.4 (a) it is also noted that the decay characteristics of TT and STT controlled jet reach the fully developed zone at X/D=9.0 and X/D=13.0 respectively. In comparison with the jet spread of uncontrolled jet and TT controlled jet, it is found that the STT controlled jet has the better potential core reduction of 89%. For Mach=0.8 in Fig.4 (b) the centerline Mach decay comparison reveals the potential core length reduction of TT and STT controlled jets are 78% and 90% respectively. The Fig.4 (c) comparison of Mach=1.0 shows the potential core reduction for TT and STT controlled jets are 82% and 85% respectively.

The centerline Mach decay plots Figs. 4 (a) – 4 (c) indicate that for all tested Mach number the decay characteristics of the controlled jet is significantly high.

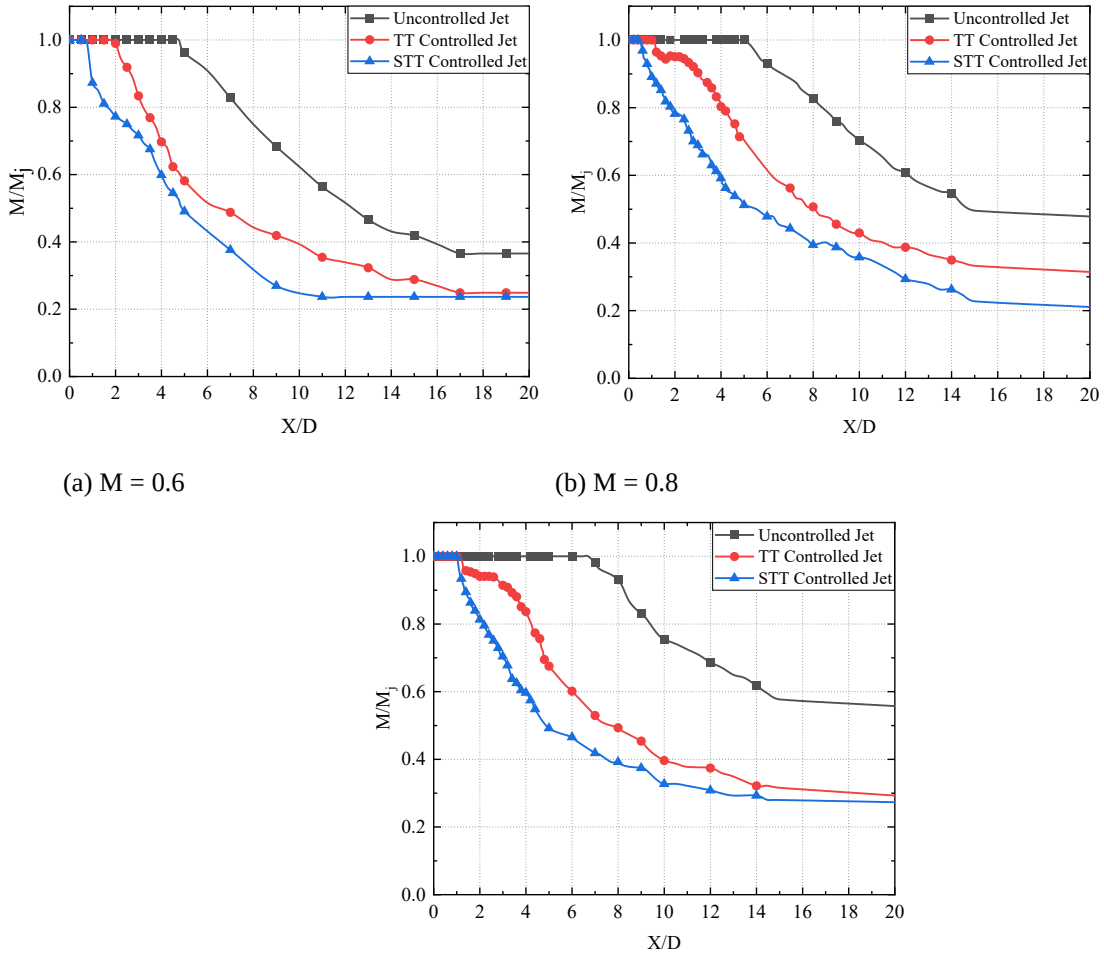

(a) M = 0.6

(b) M = 0.8

(c) M = 1.0

Fig. 4 (a) – (c) Centerline Mach decay comparison of Uncontrolled, TT controlled and STT controlled jet for various Mach Numbers

This is caused due to the creation of pair of streamwise vortices from the tab placed at the nozzle exit (Zaman, 1993). Though TT configuration also has two tabs of equal heights and is arranged in a tandem manner, the pressure uphill is created only in the first tab and the second tab is in the wake region of the first tab. The single pressure uphill created in the TT creates only one pair of vortices. The STT configuration has two tabs of unequal heights arranged in a tandem manner, flow from the nozzle exit hits the surface of both tabs and becomes stagnant at the surface of the tabs. The flow turns around the tab as there exists a low pressure or wake region behind the tab. The high pressure region formed due to the flow deceleration by the first tab is termed as pressure hill and the pressure uphill formed is proportional to the height of the tab. Since the second tab is attached to the first tab through a horizontal stem that runs to a distance equal to the width of the tab which is 3mm and the tab is arranged such that, the length of the second tab is twice the length of the first tab, similar pressure uphill is formed at the second tab at a distance of 5mm from the first tab. It is well established that the presence of pressure uphill on one side of the tab and the presence of wake region on the other side of the tab are the causes of the formation of streamwise vortices. Therefore, STT creates the formation of two uphill and two wake regions which in turn creates two sets of vortices in downstream. Hence, two sets of counter rotating streamwise vortices are created from the first tab and the second tab at two different locations and also at two different heights in the core region. These two sets of counter rotating vortices are now prevalent inside the jet stream travels further increasing the mass entrainment into the jet. Therefore, in STT the vortex is created at different tab heights and locations are responsible for the increased rate of entrainment as observed in the Fig. 4 (a)-(c). This is in accordance with the phenomenon of vortex generation from a single tab due to the formation of pressure uphill (Thanigaiarasu et al. 2020).

3.2 Radial Jet Spread Along the Tab Direction (Y/D)

The radial jet spread is plotted along the Y/D radial direction and M/M_j. The uncontrolled jet has the same radial spread along Y/D and Z/D directions since the mass entrainment is almost uniform, along the radial directions. Figure 5 (a) – (c) shows the radial jet spread characteristics of uncontrolled jets for Mach 0.6, 0.8 and 1.0. The Y/D plot for various X/D=0.25, 0.5, 1.0, 2.5, 5.0 and 10.0 locations measured from the nozzle exit shows the extent of jet spread. For each X/D, the peak velocity is located at the center of the free jet. For Mach 0.6, the Y/D radial plot for free jet in Fig. 5(a) shows the X/D=0.25 – 2.5 has peak velocity M/M_j=1.0 indicating the jet potential core is extending till X/D=2.5. Fig. 5(b) shows the radial spread of the free jet for Mach 0.8, the peak velocity M/M_j =1.0 extends till X/D=5.0.

Figure 5(c) also shows the potential core is extending till X/D=5.0. The peak velocity at X/D=10 in Fig 5 (a) – (c) shows the M/M_j value is 0.62, 0.70 and 0.71 for Mach 0.6, 0.8 and 1.0 respectively.

The Y/D radial spread for TT controlled jet Fig. 6 (a) – (c) shows the reduction of peak velocity reduction at

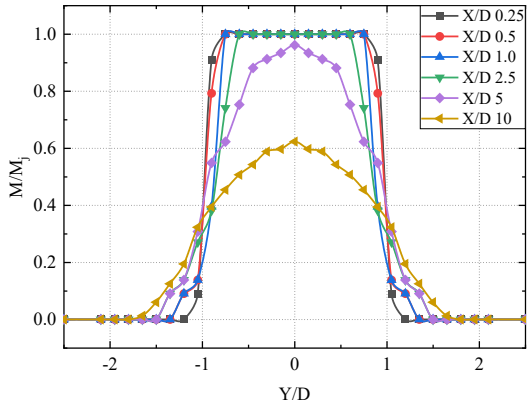

(a) M = 0.6

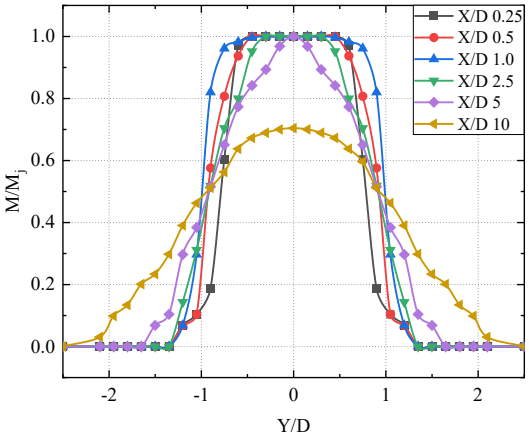

(b) M = 0.8

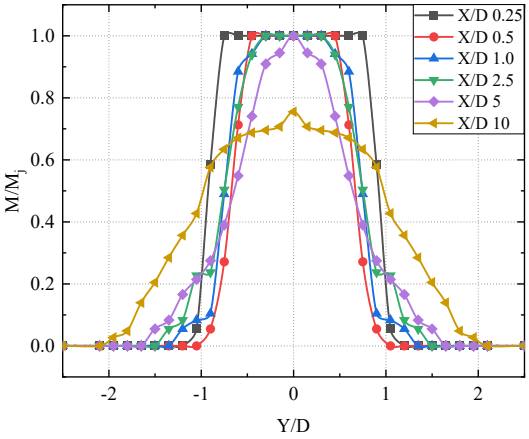

(c) M = 1.0

Fig. 5 (a) – (c) Y/D radial spread of Uncontrolled jet for various Mach Numbers

various X/D locations. The Fig. 6(a) for Mach 0.6 shows the potential core is extending till X/D=1.0 with maximum spread occurring at X/D=10 with lowest peak velocity of M/M_j = 0.4. For Mach 0.8 the Y/D radial plot in the Fig. 6(b) shows that the X/D=0.25 – 1.0 has peak velocity M/Mj=1.0 indicating the jet potential core is extending till X/D=1.0. Figure 6(c) shows the radial spread of the TT controlled jet for Mach=1.0, the peak velocity M/Mj =1.0 extends till X/D=1.0.

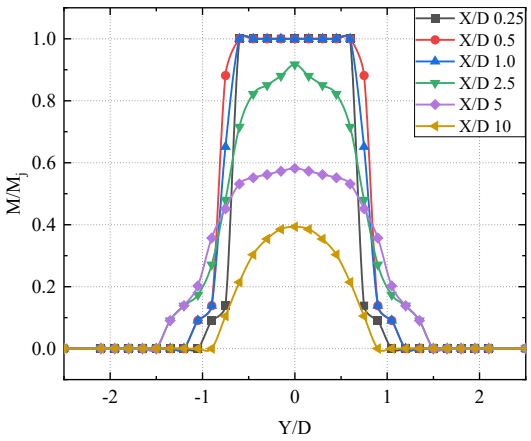

(a) M = 0.6

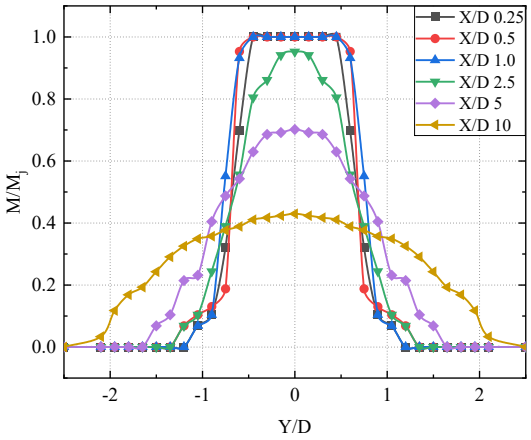

(b) M = 0.8

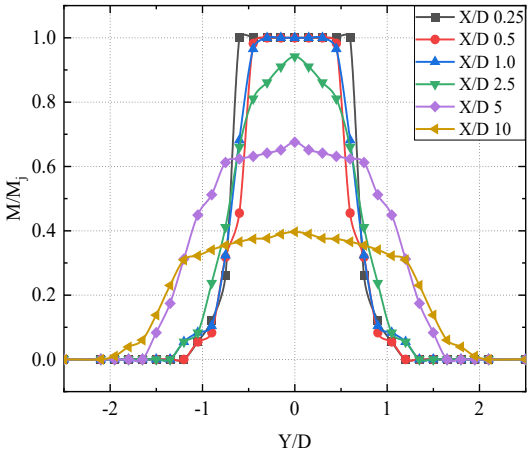

(c) M = 1.0

Fig. 6 (a) – (c) Y/D radial spread of TT controlled jet for various Mach Numbers

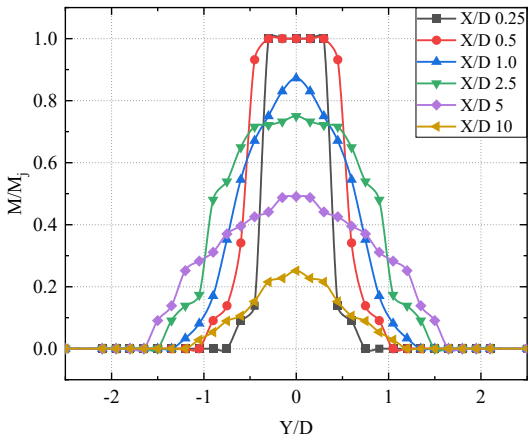

Fig. 7(a) M = 0.6

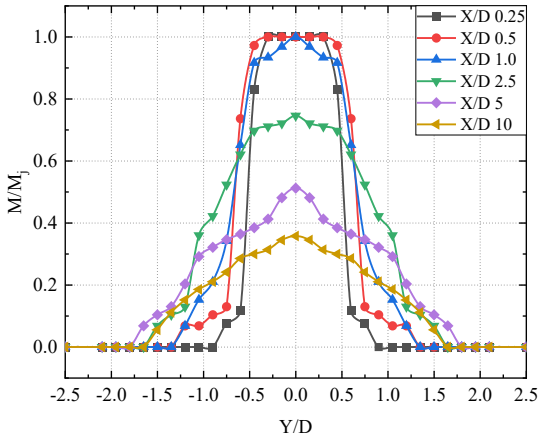

Fig. 7(b) M = 0.8

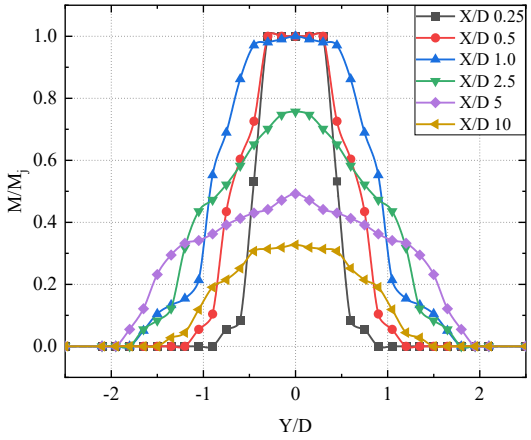

Fig. 7(c) M = 1.0

Fig. 7 (a) – (c) Y/D radial spread of STT controlled jet for various Mach Numbers

Figure 6(a) – (c) also shows the spread in the Y/D directions through the width of the plot at each X/D. For X/D=10 the width of the jet spread for Mach=0.6 is 0.75D on both sides of the jet centreline, whereas the spread is more than 2D for Mach=0.8 and 1.0.

Figure 7 (a) – (c) shows the Y/D radial spread for STT controlled jet at various X/D locations. Fig. 7(a) shows the radial spread of the STT controlled jet for Mach 0.6, the peak velocity M/Mj =1.0 extends till X/D=0.5. Fig. 7(b) for Mach=0.8 shows the extension potential core X/D=1.0 with maximum spread occurring at X/D=10 with the lowest peak velocity of M/M$_j$ = 0.25.

For Mach 1.0 the Y/D radial plot in Fig. 7(c) shows that the X/D=0.25 – 1.0 has peak velocity M/Mj=1.0 indicating the jet potential core is extending till X/D 1.0. Fig 7(a) – (c) also shows at the X/D=10 the width of the jet spread for Mach=0.6 is 1.0 D on both sides of the jet centreline, whereas the spread is more than 1.5 D for Mach=0.8 and 1.0. Figures 5-7 reveals that the exhaust jet Mach number influences the jet evolution processes. Though the characteristics of the jet for the controlled

and uncontrolled jets are similar but they are different in magnitude which is an indication of entrainment characteristics. Jet with tandem tab almost acts like a single tab configuration but the stem joining the two tabs runs along the longitudinal direction also makes contributes to the entrainment whereas, in the case of stepped tandem tabs, the presence of pressure uphill at two different locations and the presence of stem joining the two tab are responsible for effective mixing enhancement.

3.3 Radial Jet Spread Normal to the Tab Direction (Z/D)

The jet spread in radial Z-direction is plotted for TT and STT controlled jets. The creation of vortices due to the tabs is more influential Z-direction increasing the radial jet spread (Zaman 1993). The radial jet spread in Z direction shows increased width of the jet spread in both TT and STT Controlled jets. One other important factor promoting the jet spread is the jet bifurcation caused due to the tabs (Dharmahinder et al. 2011). The Z-direction radial plot of the controlled jet shows twin peak velocities indicating the bifurcation of the jet core.

Figure 8 (a) – (c) shows the radial spread along the Z-direction for TT controlled jet. Fig 8 (a) shows that the TT controlled jet for Mach=0.6 has the formation of two peaks from X/D=2.5 onwards. Though the jet has twin peaks, the peak velocity is lesser in comparison with the uncontrolled jet. For X/D=5 the peak velocity of the uncontrolled jet is M/M_j=1.0, whereas for the TT controlled jet it is M/M_j=0.78. Therefore, the reduction in peak velocities for Mach=0.6 at X/D=5 is 22%, indicating better jet decay along the Z-direction.

For Mach 0.8 the Z/D radial plot in Fig 8 (b) also exhibits the formation of two peaks due to the bifurcated jet. In comparison with the uncontrolled jet, the TT Controlled jet shows 24% reduction in the peak velocity at X/D=10. Figure 8(c) plotted for exit Mach 1.0 shows the TT controlled jet has 33% reduction in the peak velocity at X/D=10.

The Z/D radial plot for STT Controlled jet is shown in Fig 9 (a) - (c). The STT controlled jet for exit Mach= 0.6, 0.8 and 1.0 shows the presence of jet bifurcation resulting in twin peaks. Fig 9 (a) for exit Mach 0.6 shows the formation of twin peaks happens at X/D=1.0 indicating the jet bifurcation starts earlier in comparison with the TT controlled jet. Also, at X/D=5 the reduction in peak is 15% in comparison with the TT controlled jets.

For exit Mach=0.8 the Z/D radial spread in Fig 9 (b) shows 20% reduction in peak velocity in comparison with the TT Controlled jet. The STT controlled jet in Fig 9(c) shows 23% reduction in peak velocity in comparison with the TT Controlled jet. The STT controlled jet in comparison with the uncontrolled jet shows peak velocity reduction of 60%, 44% and 56% for Mach=0.6, 0.8 and 1.0 respectively. The Z/D radial plot for STT controlled jet shows dominant spread characteristics occurring due to the reduced peak velocity at all X/D locations.

The Y/D and Z/D radial plots indicate that the mixing characteristics of STT controlled jets are superior to

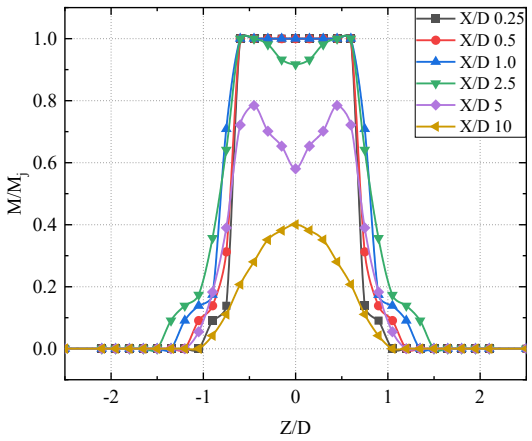

(a) M = 0.6

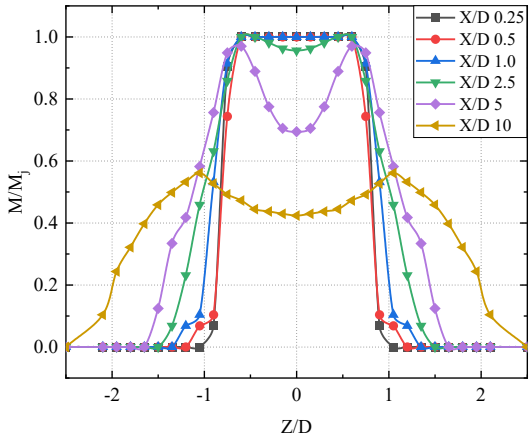

(b) M = 0.8

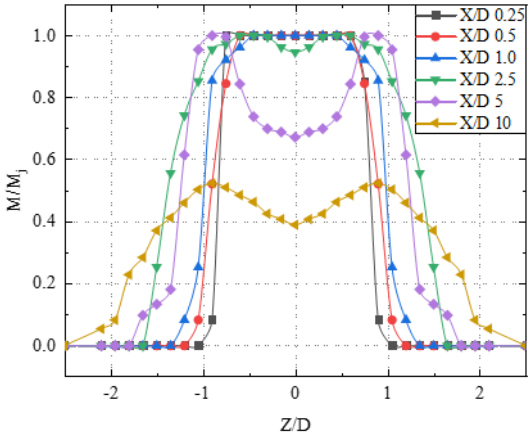

(c) M = 1.0

Fig. 8 (a) – (c) Z/D radial spread of TT controlled jet for various Mach Numbers

uncontrolled and TT Controlled jet. Aligned with the understanding of Dharmahinder et al. (2011) that the generation of multiple vortices of varying size promotes more mixing in the jet.

The Y/D and Z/D radial plots reassure that the STT controlled jet possesses higher jet mixing characteristics; this might be due to its capability of creating two pressure up-hills ahead of each tab. The vortices sourced from these pressure hills will travel downstream and increases the mass entrainment into the jet stream. From

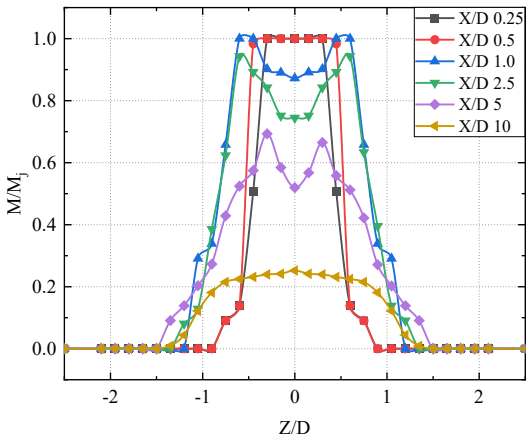

(a) M = 0.6

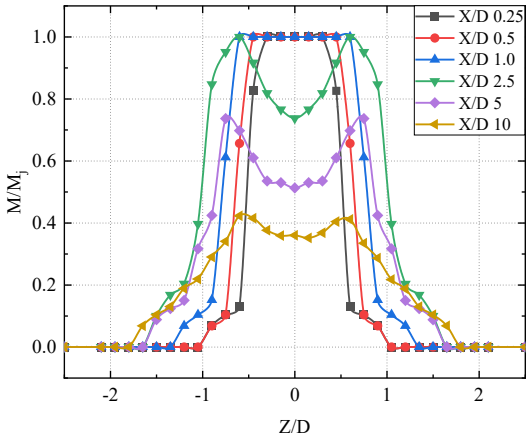

(b) M = 0.8

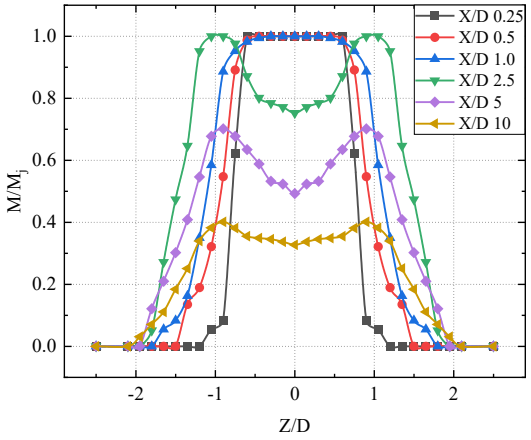

(c) M = 1.0

Fig. 9 (a) – (c) Z/D radial spread of STT controlled jet for various Mach Numbers

the radial jet spread plots, it is evident that the STT configuration creates more vortices and results in better mixing characteristics.

The Single tab and Tandem tab are found to have different wake behaviors. In the Tandem Tab, the distance between the two tabs is designed to be equal to the width of the tab which is close to the agreement of Auteri et al. (2008) for better vortex generation.

In the TT configuration, the shear layer originating from the first tab bypasses the second tab and rolls after

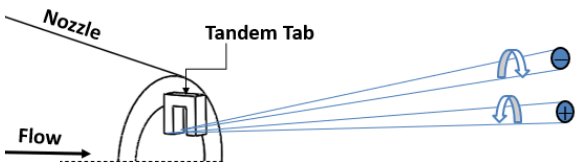

a

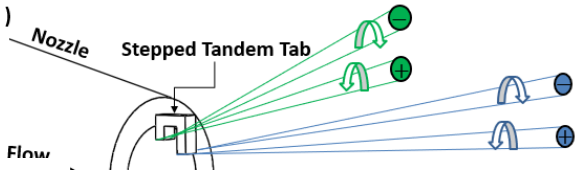

b

Fig. 10 Streamwise vortices generation (a) TT Controlled Jet, (b) STT Controlled Jet

the second tab as shown in Fig. 10(a). Hence the performance of the single tandem and tandem tab with the same height is predicted to be equal.

But in the STT the reduced height of the first tab will ensure the formation of flow stagnation on both first and second tab surfaces. This will create one shear layer originating from the first tab and another shear layer originating from the second tab with delayed time intervals. The two shear layers from the STT configuration will create two transverse vortices which will transform into streamwise vortices while traveling downstream as shown in Fig. 10(b). The two vortex systems may also interact with each other thus creating more unsteadiness and better mixing characteristics in the jet stream. The formation of vortices of varying sizes from the STT configuration will increase the mass entrainment thus promoting the jet mixing (Rathakrishnan, 2019). The time delay in the formation of vortices could also be the reason for the STT configuration to have enhanced jet mixing characteristics.

4. SIMULATION AND VALIDATION

The preliminary computational analysis of the flow field for exit Mach number M_j=0.8 is carried out for Uncontrolled, TT controlled and STT controlled jet using Ansys Fluent 16. The Ansys Fluent is chosen for its wide range of applications and versatility to post-process the solutions. The three-dimensional computational domain shown in Fig. 11 with size 30 D in radial direction and 60 D in length is chosen to capture the entire jet spread. The inlet boundary condition is defined as the pressure inlet in accordance with the experimentation. The settling chamber pressure in the experiment is set as the inlet pressure for the nozzle intake. The exit conditions and wall are defined as pressure outlet and non-slip conditions respectively. The turbulence model is chosen to be Spalart-Allmaras which is used widely for the jet study (Reddy & Zaman, 2006; Thanigaiarasu et al., 2023). The SIMPLE algorithm is used for coupling the pressure and velocity terms. The second-order upwind

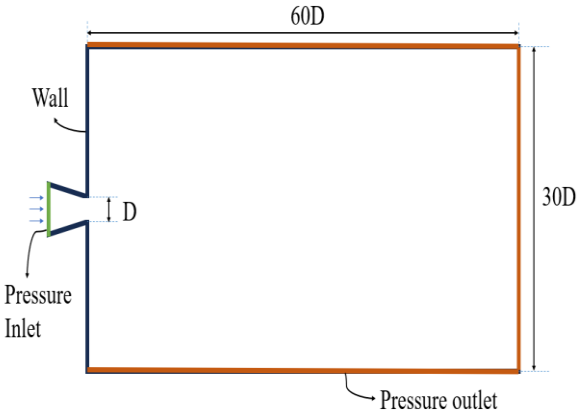

Fig. 11 Computational domain and the boundary conditions

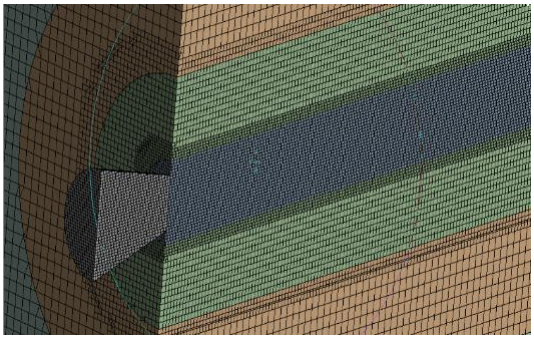

Fig. 12(a) Structured mesh for Uncontrolled jet

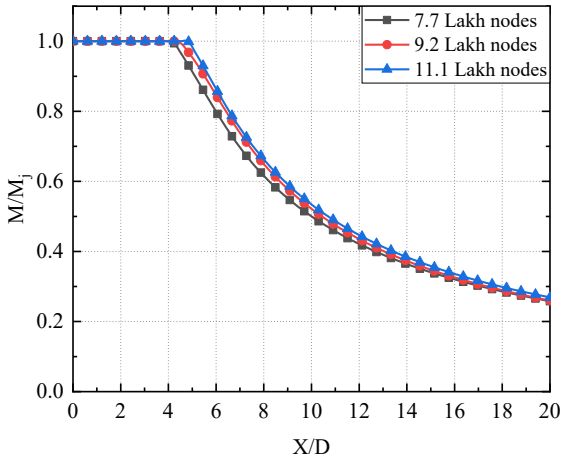

Fig. 12(b) Grid independence for varying mesh size

differencing scheme is used for the turbulence quantities to enhance the accuracy of the computational results. A multi-block structured mesh shown in Fig. 12(a) is used for discretizing the domain.

The turbulence equations of the Spalart-Allmaras model written in terms of eddy viscosity Eq. (1) – (8) are as follows (Wilcox, 1993).

Kinematic Eddy Viscosity

$$v_T = \overline{v}\, f_{v1} \tag{1}$$

Eddy Viscosity Equation

$$\frac{\partial \overline{v}}{\partial t} + U_j \frac{\partial \overline{v}}{\partial x_j} = c_{b1}\tilde{S}\overline{v} - c_{w1} f_w \left(\frac{\overline{v}}{d}\right)^2 + \frac{1}{\sigma}\frac{\partial}{\partial x_k}\left\{v\overline{v}\frac{\partial \overline{v}}{\partial x_k}\right\} + \frac{c_{w1}}{\sigma}\left(\frac{\partial \overline{v}}{\partial x_k}\right)^2 \tag{2}$$

Closure Coefficients

$$c_{b1} = 0.1355,\ c_{b2} = 0.662,\ c_{v1} = 7.1,\ \sigma = 2/3 \tag{3}$$

$$c_{w1} = \frac{c_{b1}}{k^2} + \frac{(1 + c_{b2})}{\sigma},\ c_{w2} = 0.3,\ c_{w3} = 2, k = 0.41 \tag{4}$$

Auxiliary Equations

$$f_{v1} = \frac{X^3}{X^3 + c_{v1}^3}, f_{v2} = 1 - \frac{X}{1 + X f_{v1}}, f_w = g\left[\frac{1 + c_{w3}^6}{g^6 + c_{w3}^6}\right]^{\frac{1}{6}} \tag{5}$$

$$X = \frac{\overline{v}}{v}, g = r + c_{w2}(r^6 - r), r = \frac{\overline{v}}{\tilde{S}k^2d^2} \tag{6}$$

$$\tilde{S} = S + \frac{\overline{v}}{k^2 d^2} f_{v2}, S = \sqrt{2\Omega_{ij}\Omega_{ij}} \tag{7}$$

The Rotation Tensor

$$\Omega_{ij} = \frac{1}{2}\left(\frac{\partial U_i}{\partial x_j} - \frac{\partial U_j}{\partial x_i}\right) \tag{8}$$

Where *d* is the distance from the closest surface.

The structured mesh provides a faster rate of convergence resulting in lower computational time. The grid independence is ensured using a centerline Mach decay plot for three distinct mesh sizes shown in Fig. 12(b). The mesh with 11.1 lakh nodes is chosen which is adequate to capture the potential core and the downstream jet spread.

The validation of the computational results for Mj = 0.8 uncontrolled jet is shown in Fig. 13. The experimentation of the uncontrolled jet earlier revealed that the potential core length is X/D = 5.0. In comparison, the computation shows that the potential core length of exit Mach number M$_j$ = 0.8 is X/D = 5.45.

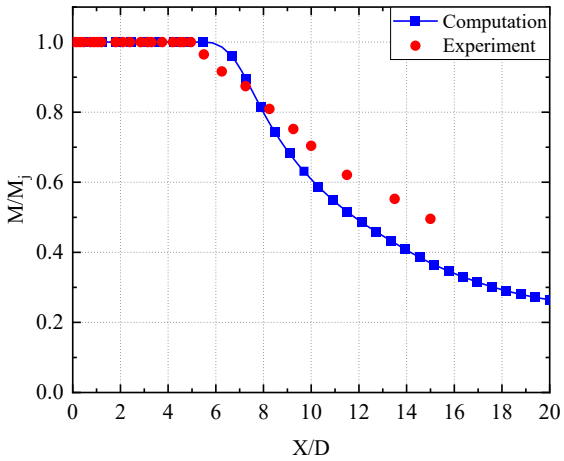

Fig. 13 Validation of Centerline Mach decay for M = 0.8

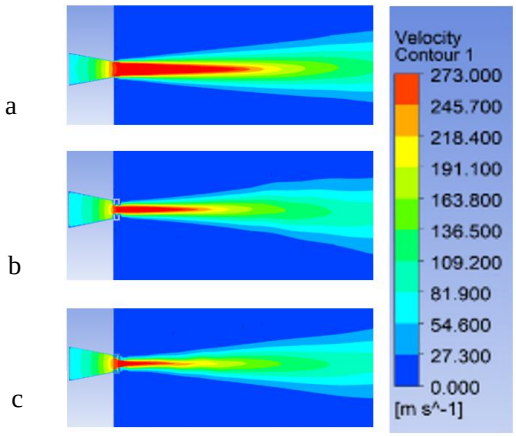

Fig. 14 Y/D radial Velocity contour (a) Uncontrolled jet, (b) TT controlled jet and (c) STT controlled jet

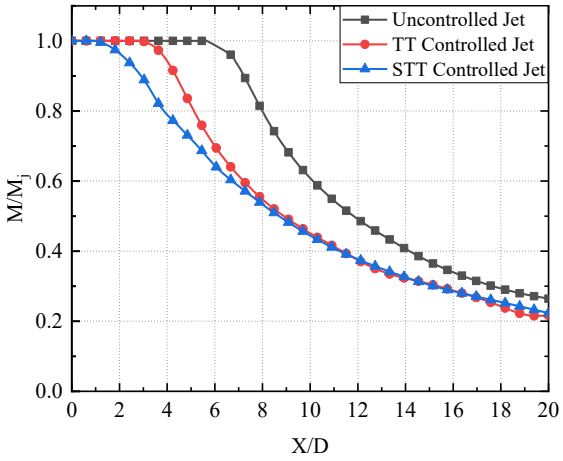

Fig. 16 Centerline Mach decay comparison through Computation, M = 0.8

The computation therefore predicts the potential core length with an accuracy of 90%. However, the downstream flow field shows that the characteristic decay is much faster in computational results. This variation could be due to the influence of the Spalart Allmaras turbulence model predicting consistently higher jet spread rates (Wilcox, 1993). The computation for TT and STT controlled jets are conducted using similar mesh generation and boundary conditions.

The computational results of the flow field TT and STT controlled jets are compared with the M_j = 0.8 uncontrolled jet. The Y/D radial velocity contours are presented in Fig. 14 (a) – (c). The flow field portrays the effect of TT and STT controlled jet on potential core reduction. It is noted that the influence of the tabs has effect on the jet spread in the Y/D radial direction. However, the STT controlled jet is found to have the least core length in comparison with the uncontrolled jet and TT controlled jet.

The Fig. 15 (a) – (c) shows the Z/D radial velocity contours and the effect of controlled jets. The TT and STT controlled jets show higher jet spread in the Z/D direction. The TT and STT controlled jet depict the bifurcation of the jet. A similar behavior of jet split was noted in experimental results shown in Fig. 8(b) and Fig. 9(b).

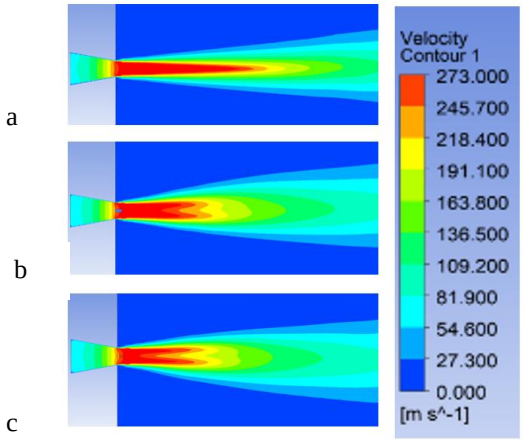

Fig. 15 Z/D radial Velocity contour (a) Uncontrolled jet, (b) TT controlled jet and (c) STT controlled jet

The comparison of centerline Mach decay for exit Mach 0.8 compared for three configurations is shown in Fig. 16. The TT controlled jet shows the potential core length extending up to X/D=2.2 providing a 61% reduction. Whereas the STT controlled jet with core length X/D=0.81 shows an 85% reduction in the potential core. The computational result shown in Fig. 16 reassures the experimental results in Fig. 4(b) on the potential core reduction using TT and STT configurations.

The computational analysis conducted for exit Mach number 0.8 reveals a strong correlation with the potential core length and radial spread of experimental results. The TT and STT controlled jets have shown higher mixing rates with a reduction in the potential core length. The STT configuration shows higher potential core reduction of 90% and 85% in studies conducted through experiments and simulation respectively. It is apparent that the STT controlled jet shows dominant spread characteristics through a stronger and preponed jet split seen in both experiment Figure 9(b) and computation Fig. 15 (c). Thus, reassuring that the STT configuration is the better mixing promoter in the aspect of both potential core reduction and radial spread.

5. APPLICATION AND LIMITATIONS

The advantages of STT jet control such as higher potential core reduction and more jet spread will provide solutions for a wide area of applications. The control methods could potentially be used to reduce the heat signatures of the nozzle exhaust. The better jet spread characteristics are applicable for areas such as augmenting combustion efficiency and reduction in jet noise. The effective mixing achieved through STT controlled jets is limited to the structural viability of the tabs. Since the tabs are introduced into the high speed and high temperature flows, the design aspects of

stiffness and vibrational characteristics are vital for their real-time applicability.

6. CONCLUSION

The experimental investigation conducted for subsonic and sonic jets reveals that the STT configuration promotes better jet mixing. The results of STT controlled jets are compared with the uncontrolled and TT controlled jets. The comparison of centerline Mach decay shows the STT controlled jets have reduced potential core of 89%, 90% and 85% for exit Mach=0.6, 0.8 and 1.0 respectively. The vortices created by the STT configuration exhibit better mass entrainment from the atmosphere to the jet core. The radial spread shows the jet bifurcation is preponed in STT controlled jets resulting in faster decay and spread of the jet. The radial spread in Y and Z directions also shows that the STT configuration produces more jet spread along with reduced peak velocity at all X/D locations. The computational analysis carried out for Mach=0.8 reassures that SST controlled jet has better mixing characteristics. The effect of the TT and STT jet controls for supersonic and under-expanded jets will be experimented in a separate study.

ACKNOWLEDGEMENTS

The authors wish to thank Dr. E. Rathakrishnan, Professor (retired), Indian Institute of Technology, Kanpur for his commendable contribution to jet mixing techniques and the experimental methodology. His work has inspired the authors to pursue the current research with ease and confidence.

CONFLICT OF INTEREST

The authors propose that there are no conflicts to disclose in the present research.

AUTHORS CONTRIBUTION

All three authors have made significant contributions towards Experimental Investigation, Research Methodology, Data curation, Visualization, Formal Analysis, Writing – Original Draft Preparation and critical revision of the article.

REFERENCES

Ahuja, K. K., & Brown W. H. (1989). Shear flow control by mechanical tabs. *AIAA*, *89*, 0994. https://doi.org/10.2514/6.1989-994

Alam, M. M., Bai, H., & Zhou, Y. (2016). The wake of two staggered square cylinders. *Journal of Fluid Mechanics*, *801*, 475–507. https://doi.org/10.1017/jfm.2016.303

Ahmed R. A., Thanigaiarasu, S., Santhosh, J., Elangovan, S., & Rathakrishnan, E. (2013). Study of slanted perforated jets, *International Journal of Turbo & Jet Engines*, *30*(4), 347–357. https://doi.org/10.1515/tjj-2013-0015

Ahmed R. A., Thanigaiarasu, S., Venkatramanan, S., Elangovan, S., & Rathakrishnan, E. (2015). *Study of slanted perforated shapes in tabs for control of subsonic Jets.* AIAA, 2015-2423. https://doi.org/10.2514/6.2015-2423

Auteri, F., Belan, M., Gibertini, G., & Grassi, D. (2008). Normal flat plates in tandem: An experimental investigation. *Journal of Wind Engineering and Industrial Aerodynamics*, *96*, 872–879. https://doi.org/10.1016/j.jweia.2007.06.014

Bohl, D. G., & Foss, J. F. (1996). *Enhancement of passive mixing tabs by the addition of secondary tabs*. *AIAA*, *96*, 0545. https://doi.org/10.2514/6.1996-545

Bradbury, L. J. S., & Khadem, A. H. (1975). The distortion of a jet by tabs. *Journal of Fluid Mechanics*, *70*(4), 801-813. https://doi.org/10.1017/S0022112075002352

Chand, D. S., Thanigaiarasu, S., Elangovan, S., & Rathakrishnan, E. (2011). Perforated arc-tabs for jet control. *Int. J. Turbo Jet-Engines*, *28*, 133-138. https://doi.org/10.1515/tjj.2011.012

Gretta, W. J., & Smith, C. R. (1993). The flow structure and statistics of a passive mixing tab. *Journal of Fluids Engineering*, 115/255. https://doi.org/10.1115/1.2910133

Jabez Richards, S. B., Thanigaiarasu, S., & Kaushik, M. (2023). Experimental study on the effect of tabs with asymmetric projections on the mixing characteristics of subsonic jets. *Journal of Applied Fluid Mechanics*, *16*(6), 1208-1217. https://doi.org/10.47176/jafm.16.06.1584

Lovaraju, P., Paparao, K. P. V., & Rathakrishnan, E. (2004). Shifted cross-wire for supersonic jet control. *AIAA*, 2004-4080. https://doi.org/10.2514/6.2004-4080

Maruthupandiyan, K., & Rathakrishnan, E. (2016). Supersonic jet control with shifted tabs. *Proceedings of the Institution of Mechanical Engineers, Part G: Journal of Aerospace Engineering*, *2018*, 232(3):433-447. https://doi.org/10.1177/0954410016679197

Singh, N. K., and Rathakrishnan E. (2002). Sonic jet control with tabs. *Journal of Turbo and Jet Engines*, *19*, 107-118. https://doi.org/10.1515/TJJ.2002.19.1-2.107

Rathakrishnan, E. (2012). Visualization of the flow fieldaround a flat plate. *IEEE Instrumentation and Measurement Magazine*, *15*(6), 8-12. https://doi.org/10.1109/mim.2012.6365535

Rathakrishnan, E. (2019). *Applied gas dynamics*. John Wiley & Sons. https://doi.org/10.1002/9781119500377.ch12

Reddy, D. R., & Zaman, K. B. M. Q. (2006). Computational study of effect of tabs on a jet in a

cross flow. *Computers and Fluids*, *35*(7), 712–723. https://doi.org/10.1016/j.compfluid.2006.01.011

Samimy, M., Zaman, K. B. M. Q., & Reeder, M. F. (1993). Effect of tabs on the flow and noise field of an axisymmetric jet. *AIAA*, *31*(4), 609–619. https://doi.org/10.2514/3.11594

Thanigaiarasu, S., Balamani, G., Mirnal, K., & Revathy, K. (2023). Computational study on the effect of vane design in enhancing the mixing of subsonic jet and sonic jet. *Journal of Applied Fluid Mechanics*, 16(12), 2316-2328. https://doi.org/10.47176/jafm.16.12.2092

Thanigaiarasu, S., Jabez Richards, S. B., Karthikeyan, V., Muthuram, A., Yadav, S. K., Vijaya Raj, T. (2020). *Numerical Study on the Effect of Innovative Vortex Generators in the Mixing Enhancement of Subsonic Jets.* Proceedings of International Conference of Aerospace and Mechanical Engineering 2019. Lecture Notes in Mechanical Engineering. Springer, Singapore. https://doi.org/10.1007/978-981-15-4756-0_35

Thanigaiarasu, S., Jayaprakash, S., Elangovan, S., & Rathakrishnan, E. (2008). Influence of tab geometry and its orientation on under-expanded sonic jets. *Proceedings of the Institution of Mechanical Engineers, Part G: Journal of Aerospace Engineering, 222(3), 331-339.* https://doi.org/10.1243/09544100JAERO299

Wilcox, D. C. (1993). *Turbulence modeling for CFD*. DCW Industries, Inc.

Zaman, K. B. M. Q. (1993). *Streamwise vorticity Generation and mixing enhancement in free jets by delta-tabs. AIAA, 93,* 3253. https://doi.org/10.2514/6.1993-3253

Zaman, K. B. M. Q., Reeder, M. F., & Samimy, M. (1992). Supersonic jet mixing enhancement by delta-tabs. *AIAA, 92,* 3548, 1992. https://doi.org/10.2514/6.1992-3548

Zaman, K. B. M. Q., Reeder, M. F., & Samimy, M. (1994). Control of an axisymmetric jet using vortex generators. *Physics of Fluids*, *6*, 778-793. https://doi.org/10.1063/1.868316